Stimulus-Specific Oscillations in a Retinal Model

Garrett T. Kenyon, Bryan J. Travis, James Theiler, John S. George, Gregory J. Stephens, and David W. Marshak

***Abstract*—High-frequency oscillatory potentials (HFOPs) in the vertebrate retina are stimulus specific. The phases of HFOPs recorded at any given retinal location drift randomly over time, but regions activated by the same stimulus tend to remain phase locked with approximately zero lag, whereas regions activated by spatially separate stimuli are typically uncorrelated. Based on retinal anatomy, we previously postulated that HFOPs are mediated by feedback from a class of axon-bearing amacrine cells that receive excitation from neighboring ganglion cells-via gap junctions-and make inhibitory synapses back onto the surrounding ganglion cells. Using a computer model, we show here that such circuitry can account for the stimulus specificity of HFOPs in response to both high- and low-contrast features. Phase locking between pairs of model ganglion cells did not depend critically on their separation distance, but on whether the applied stimulus created a continuous path between them. The degree of phase locking between spatially separate stimuli was reduced by lateral inhibition, which created a buffer zone around strongly activated regions. Stimulating the inhibited region between spatially separate stimuli increased their degree of phase locking proportionately. Our results suggest several experimental strategies for testing the hypothesis that stimulus-specific HFOPs arise from axon-mediated feedback in the inner retina.**

***Index Terms*—Gamma oscillations, phase locking, synchrony, temporal code segmentation.**

I. Introduction

GANGLION cells, the output neurons of the retina, represent local stimulus properties, such as contrast, as changes in their firing rates. In addition, ganglion cells may encode global stimulus properties, such as connectedness, via coherent oscillations. Large stimuli can evoke high-frequency oscillatory potentials (HFOPs) in mammalian retinas at frequencies between 60–120 Hz [2], [10], [19], [21], [22], [24], and similar oscillations have been recorded in cold-blooded vertebrates at lower frequencies [13], [28]. HFOPs are also present in electroretinograms (ERGs) of humans [7], [27] and other primates [11], [23]. The phylogenetic conservation of HFOPs across vertebrate retinas suggests they may be important for visual function.

Manuscript received June 1, 2003; revised December 23, 2003. This work was supported in part by the Department of Energy Office of Nonproliferation Research and Engineering, in part by the Mental Illness and Neurological Discovery (MIND) Institute for Functional Brain Imaging, Alburquerque, NM, and in part by the Lab Directed Research and Development Program at Los Alamos National Laboratory. The work of D.W. Marshak was supported by the National Eye Institute under Grant EY06472 and the National Institute of Neurological Disease and Stroke under Grant. NS38310.

G. T. Kenyon, B. J. Travis, J. Theiler, J. S. George, and G. J. S. Stephens are with the Los Alamos National Laboratory, Los Alamos, NM 87545 USA (e-mail: gkeyon; bjtravis; jt; jsg; gstephens@lanl.gov).

D. W. Marshak is with the Department of Neurobiology and Anatomy, University of Texas Medical School, Houston, TX 77030 USA (e-mail: David.W.Marshak@uth.tmc.edu).

Digital Object Identifier 10.1109/TNN.2004.832722

In those retinal preparations where the question of stimulus specificity has been directly investigated, primarily in the frog [13] and cat [22], HFOPs have been shown to be stimulus specific. Oscillations arising from regions activated by the same contiguous stimulus are phase locked with approximately zero lag, even though the phase itself varies randomly over time relative to the stimulus onset. Oscillations arising from regions activated by spatially separate stimuli, however, are temporally uncorrelated.

We previously proposed that negative feedback from axon-bearing amacrine cells, inhibitory interneurons, produces oscillatory responses that might underlie HFOPs [15], [16]. According to this hypothesis, the dendrites of axon-bearing amacrine cells are excited by neighboring ganglion cells via gap junctions and their axons provide feedback inhibition to more distant ganglion cells. This connectivity is consistent with patterns of ganglion cell tracer coupling [6], [14], [26], electron microscopy of gap junction contacts between ganglion and amacrine cells [14], and with the distribution of synaptic contacts made by wide-field amacrine cells [9], [18].

Here, we used a computer model of the inner retina to characterize the stimulus specificity of HFOPs produced by axon-mediated feedback. An integrate-and-fire process was used to describe the behavior of spiking neurons and a stochastic process to describe the effects of transmitter release from nonspiking neurons. Ganglion cells were modeled as cat alpha (Y) ganglion cells, based on physiological evidence that alpha ganglion cells fire synchronously [3], [20]. Previous modeling studies have shown that axon-mediated feedback can produce physiologically realistic HFOPs consistent with the temporal dynamics and center-surround organization of cat retinal ganglion cells [16]. Moreover, these axon-mediated HFOPs were robust to changes in individual parameters and to changes in the numerical precision of the integration routine [16].

The principal findings reported here are: 1) phase locking of retinal HFOPs produced by axon-mediated feedback does not depend critically on the distance between the recorded cells but on whether there exists a continuously stimulated path between them (i.e., whether the corresponding points in the image belong to a single, contiguous visual feature); 2) phase locking falls off abruptly as the end-to-end distance between two bar stimuli increases, illustrating the pivotal role of gap junctions in synchronizing HFOPs within contiguously activated regions; and 3) HFOPs become less specific for stimulus configurations in which large numbers of axons cross between activated regions, such as commonly occurs in natural scenes where overlapping objects are often separated by a long low-contrast border. Together, these findings provide several experimentally testable predictions for investigating the hypothesis that feedback circuitry in the inner retina, consisting of local excitation via gap

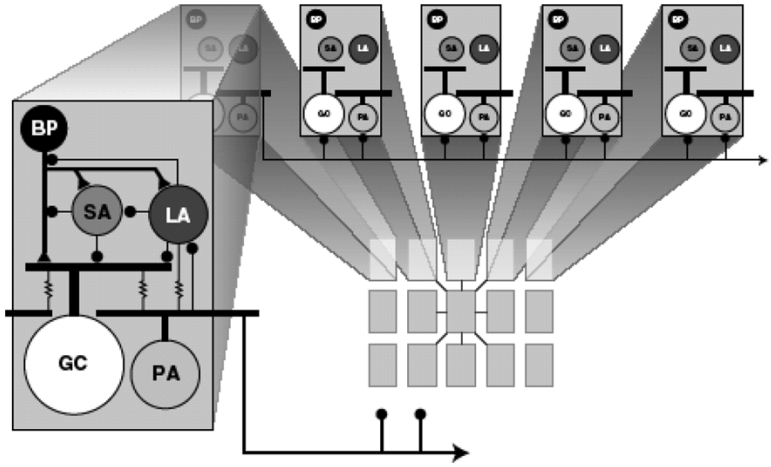

Fig. 1. Cell types and major connections in the retinal model illustrated at three spatial scales. The model consisted of a 32 × 32 array of identical local processing modules consisting of five cells types: bipolar (BP) cells, small (SA), large (LA) and poly-axonal (PA) amacrine cells, and alpha ganglion (GC) cells. In each local module, there were four BPs, four SAs, four PAs, one LA, and one GC (only one cell of each type is depicted). Local Connections: the BPs excited all four third-order cell types, but their input to the PAs was very weak (not all connections depicted). Amacrine cells made three kinds of local inhibitory connections: feedforward inhibition of the GCs, feedback inhibition of the BPs, and serial inhibition among themselves. The PAs were coupled by gap junctions to the GCs, the LAs, and to each other. Long-Range Connections: the PAs gave rise to long axons that inhibited all cell types in the surrounding area, but most strongly contacted the GCs and other PAs. Explanation of symbols: excitation (triangles), inhibition (circles), gap junctions (resistors).

junctions combined with long-range axon-mediated inhibition, underlies the temporal coding of topological information in the optic nerve. A preliminary report of these results has appeared previously [17].

II. Methods

A. Model Overview

The model retina consisted of five parallel interconnected two-dimensional (2-D) grids, one for each cell type (Fig. 1). The model bipolar cells produced excitatory postsynaptic potentials (EPSPs) in both ganglion cells and amacrine cells according to a random process [8]. EPSPs were balanced by inhibitory post-synaptic potentials (IPSPs) from three different amacrine cell types encompassing three different spatial scales, which are: 1) small amacrine cells whose dendritic fields were the same size as those of the bipolar cells; 2) large amacrine cells whose dendritic fields were the same size as those of the ganglion cells; and 3) axon-bearing amacrine cells, whose dendritic fields were the same size as those of the bipolar cells but whose axonal connections spread out over a large retinal area. Of the three amacrine cell types in the model, only the axon-bearing amacrine cells fired spikes. All three amacrine cell types made feedforward synapses onto ganglion cells, feedback synapses onto bipolar cells, as well as serial synapses among themselves.

B. Simulation

All cell types were modeled as single compartment, RC circuit elements obeying a first-order differential equation of the following form: see (1) , shown at the bottom of the page, where $\{V^{(k)}\}$ is a 2-D array denoting the normalized membrane potentials of all cells of type k, $1 \leq k \leq 5$, $\tau^{(k)}$ are the time constants, $b^{(k)}$ are bias currents, $\{L^{(k)}\}$ are 2-D arrays representing light stimulation ($\{L^{(k)}\} = 0, k \neq 1$), $\{W^{(k,k')}\}$ gives the connection strengths, implemented as Gaussian functions of the Euclidian distance between presynaptic, k', and postsynaptic, k, cell types, and the functions $f^{(k,k')}$ give the associated input–output relations. The weight matrices, $\{W^{(k,k')}\}$, and the input–output relations, $f^{(k,k')}$, are described in greater detail below. The output of the axon-mediated inhibition was delayed by 2 ms, except for the axonal connections onto the axon-bearing amacrine cells, which was delayed for 1 ms. This difference in conduction delays resulted from limitations imposed by the original implementation of the simulator. Subsequent studies, using a more advanced simulator, confirmed that similar results to those reported here are obtained when a physiologically realistic model of axon conduction delays is employed [16]. All other synaptic interactions were delayed by one time step, equal to 1 ms, representing a typical rise-time for PSPs. Equations were integrated using a direct Euler method. Separate control studies confirmed that the model exhibited similar behavior regardless of the integration step size as long as the finite PSP rise time was modeled explicitly [16].

The input–output function for gap junctions was given by the identity

$$f^{(k,k')}\left(\overleftrightarrow{V}^{(k')}\right) = \overleftrightarrow{V}^{(k')} \tag{2}$$

$$\dot{\overleftrightarrow{V}}^{(k)} = -\frac{1}{\tau^{(k)}}\left(\begin{array}{c} \overleftrightarrow{V}^{(k)} - b^{(k)} - \overleftrightarrow{L}^{(k)} \\ -\sum_{k'} \overleftrightarrow{W}(k,k') \cdot f^{(k,k')}\left(\overleftrightarrow{V}^{(k')}\right) \cdot \overleftrightarrow{W}^{(k,k')^T} \end{array}\right) \tag{1}$$

where the dependence on the presynaptic potential has been absorbed into the definition of $\tau^{(k)}$.

The input–output function for graded stochastic synapses that did not require action potential spikes to produce PSPs was constructed by comparing, on each time step, a random number with a Fermi-function

$$f^{(k,k')}\left(\overset{\leftrightarrow}{V}^{(k')}\right) = \theta\left(\left[\frac{1}{1+\exp\left(-\alpha\overset{\leftrightarrow}{V}^{(k')}\right)}\right] - r\right) \quad (3)$$

where α sets the gain (equal to 4), r is a uniform random deviate equally likely to take any real value between 0 and 1, and θ is a step function $\theta(x) = 1, x > 0; \theta(x) = 0, x \leq 0$.

Finally, the input–output relation used to describe the conventional synapses made by the spiking axon-bearing amacrine cells was

$$f^{(k,k')}\left(\overset{\leftrightarrow}{V}^{(k')}\right) = \theta\left(\overset{\leftrightarrow}{V}^{(k')}\right). \quad (4)$$

A modified integrate-and-fire mechanism was used to model spike generation. A positive pulse (amplitude $= 10.0$) was delivered to the cell on the time step after the membrane potential crossed threshold, followed by a negative pulse (amplitude $= -10.0$) after a delay of 1 ms. It was necessary to explicitly model action potentials as these could affect neighboring cells via gap junctions. The bias current b, was incremented by – 0.5 following each spike, and then decayed back to the resting value with the time constant of the cell, representing a relative refractory period.

Synaptic weights were modeled as separable Gaussian functions, with the total weight given by the product of two terms representing the dependence on either the horizontal (columns) or vertical separation (rows) between pre- and post-synaptic elements. The horizontal weight factor $\{W^{(k,k')}\}_{i(k),j(k')}$ was determined by a Gaussian function of the following:

$$W^{(k,k')}_{i^{(k)},j^{(k')}} = \alpha\sqrt{W^{(k,k')}}e^{-\left[||i^{(k)}-j^{(k')}||^2/2\sigma^2\right]} \quad (5)$$

which gives the synaptic weight between the presynaptic location $j^{(k')}$ (the jth column in the array of cells of type k') to the postsynaptic location $i^{(k)}$ (the ith column in the array of cells of type k), α is a normalization factor which ensured that the total integrated synaptic input equaled $W^{(k,k')}$, σ is the Gaussian radius of the interaction, and the quantity $||i^{(k)}-j^{(k')}||$ denotes the horizontal distance between the pre- and post-synaptic columns, taking into account the wrap around boundary conditions employed to mitigate edge effects. An analogous weight factor describes the dependence on the row separation.

The spatial extent of synaptic interactions depended on the input and output radii of the post- and presynaptic cell types, respectively. Specifically, (5) was augmented by a cutoff condition that prevented synaptic interactions beyond a specified distance, determined by the radius of influence of the presynaptic outputs and the postsynaptic inputs, corresponding to the axonal and dendritic fields, respectively. A synaptic connection was only possible if the output radius of the presynaptic cell overlapped the input radius of the postsynaptic cell. Except for the long distance connections made by the axon-bearing amacrine cells, the input and output radii were equal, reflecting the fact that in the retina the same processes are typically both pre- and postsynaptic. For the large amacrine cells and the ganglion cells, the radius of influence extended out to the centers of the nearest neighboring cells of the same type. The radii of the bipolar, small, and axon-bearing amacrine cells (nonaxonal connections only) extended only halfway to the nearest cell of the same type. Values for model parameters are listed in Tables I and II.

TABLE I
CELLULAR PARAMETERS

	τ	b	n×n	d	σ
BP	10.0	–0.0	64×64	0.25	0.25
SA	25.0	–0.5	64×64	0.25	0.25
LA	20.0	–0.25	32×32	1.0	0.5
PA	5.0	–0.025	64×64	0.25/9.0[a]	0.25/3.0[a]
GC	5.0	–0.025	32×32	1.0	0.5

Explanation of symbols: τ: time constant (ms); b: bias; $n \times n$: array size; d: cutoff radius, σ: Gaussian radius (see (5). [a] Inner radius/outer radius.

TABLE II
SYNAPTIC WEIGHTS

	L	BP	SA	LA	PA	GC
BP	3.0[a]	*	-0.375[b]	3.0[b]	–3.0[b]/–15.0c	*
SA	*	3.0[b]	*	-3.0[b]	0.0[b]/–15.0[c]	*
LA	*	3.0[b]	*	0.25[a]	–3.0[a]/–15.0[c]	*
PA	*	0.75[b]	–0.75b	0.25[a]	0.25[a]/–45.0[c]	0.25[a]
GC	*	9.0[b]	–4.5b	–4.5[b]	0.25[a]/–270.0[c]	*

Each term represents the total integrated weight (the quantity $W^{(i,i')}$ in (5) from all synapses arising from the corresponding presynaptic type (columns) to each cell of the corresponding postsynaptic type (rows). The first column labeled **L** denotes connections made by the external stimulus. Asterisks (*) indicate the absence of a corresponding connection. Synapse type indicated by superscript: [a] gap junction, [b] graded synapse, [c] conventional synapse. [d] Maximum coupling efficiency (ratio of post- to pre-synaptic depolarization) for this gap junction synapse: DC $= 11.3\%$, Action Potential $= 2.7\%$.

C. Data Analysis

Cross correlation histograms (CCHs) between model ganglion cells were computed from pairs of binary spike trains and the result expressed as a fraction of the baseline synchrony (correlation amplitude at zero delay in the absence of a stimulus). The correlations between spike trains drawn from different stimulus trials (shift predictors) were used to estimate the contribution from stimulus coordination [12]. CCHs were plotted as a function of the delay after averaging over all events occurring during the plateau portion of the response (200–600 ms). For each delay value, this average was compensated for edge effects arising from the finite length of the two spike trains. All rate and correlation measures, unless otherwise noted, were obtained by averaging over 200 stimulus trials, using a bin width of 1 ms. Distances within the model retina are reported in units of ganglion cell receptive field diameters, equivalent to the center-to-center separation between nearest neighbor pairs.

D. Stimuli

Input to the model consisted of external currents representing light-modulated synaptic input from cone photoreceptors. External currents were processed through a temporal low-pass filter with a time constant of 10 ms, but were not spatially filtered. Fixed-light spots were modeled as constant input currents with step onsets and sustained durations of 600 ms.

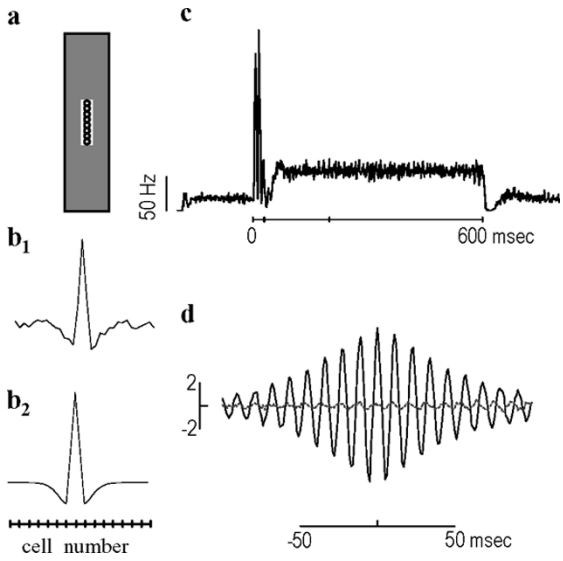

Fig. 2. Stimulus-evoked HFOPs. (a) Column of eight model ganglion cells stimulated by a narrow bar (intensity $= 1/2$). (b1) Plateau firing rates of ganglion cells along horizontal cross section through the center of the stimulus (intensity $= 1/16$). (b2) Response profile predicted by a difference-of-Gaussians (DOG) model. (c) Averaged PSTH of all stimulated cells. Solid line indicates the stimulus duration. Vertical ticks denote the peak and plateau portions of the response (bin width, 1 ms). (d) Solid black line: averaged CCH of all stimulated cell pairs. Dashed gray line: shift predictor. Only the time varying component of the shift predictor is plotted. Ganglion cells are synchronized by a fast oscillation (95 Hz) that is not phase locked to the stimulus onset.

III. Results

A. HFOPs

A narrow bar centered over a column of eight model ganglion cells [Fig. 2(a)] was used to simulate light responses. The response profile showing the plateau firing rate (plateau period; 200–600 ms) of the ganglion cells along a horizontal cross section passing through the middle of the stimulus [Fig. 2(b)] was in qualitative agreement with the response profile predicted by a two-parameter difference-of-Gaussians (DOG) model [Fig. 2(b)] whose relative center-surround strengths were fixed at their published values [25]. The averaged PSTH generated by the model [Fig. 2(c)], obtained by combining the individual PSTHs over all eight stimulated cells, exhibited a phasic-tonic profile typical of cat retinal ganglion cells [4]. Basic characteristics of the model ganglion cells, particularly their center-surround receptive field organization and phasic-tonic response dynamics, were thus qualitatively consistent with retinal physiology.

HFOPs were clearly evident in the averaged CCH recorded during the plateau portion of the response (Fig. 2(d), solid black line). The averaged CCH was computed by combining the individual CCHs computed from all distinct pairs of ganglion cells activated by the stimulus, with the total correlation strength expressed as a fraction of the expected synchrony due to chance. In all cases, shift predictors were negligible (Fig. 2(d), dashed gray line). The overall shape of the averaged CCH, particularly the oscillation frequency, the relative magnitude of the central peak, and the envelope characterizing the persistence of firing correlations with increasing delay, was quantitatively similar to the correlations computed from multiunit spike trains recorded in the cat retina in response to large spots [22]. In the model, temporal correlations peaked at zero delay, whereas small phase shifts on the order of a few milliseconds have been reported in CCHs measured physiologically [22]. Such small phase shifts could result from the natural variability in the cellular and synaptic properties of retinal neurons, a feature not accounted for in the present model in which all ganglion cells were identical.

Oscillatory activity was not evident during the plateau portion of the averaged PSTH, although periodic structure was quite prominent in the averaged CCH recorded during the same plateau portion of the response. The phases of retinal HFOPs drift randomly over time, as revealed by the decline in temporal correlations with increasing delay (reduced height of successive side peaks in the averaged CCH), causing periodic structure to be suppressed in stimulus-locked multitrial averages such as the PSTH. Increasing the stimulus size and/or intensity increased the persistence of high-frequency temporal correlations, and under these circumstances periodic structure was present in the plateau portion of the PSTH (not shown). Consistent with this observation, HFOPs can persist in the PSTHs recorded from cat retinal ganglion cells for hundreds of milliseconds following the onset of a large spot [21], whereas small spots or fine wavelength gratings do not evoke HFOPs [2], [13], [21].

To investigate how the phase locking of HFOPs depended on the distance between recording locations in the retinal model, CCHs were evaluated for ganglion cell pairs arranged symmetrically about the center of a narrow bar stimulus using data from the plateau portion of the response (Fig. 3). Regardless of spatial separation, the individual CCHs recorded in response to a bar stimulus were similar to the averaged CCH shown in Fig. 2, demonstrating that HFOPs in the retinal model could remain phase locked over considerable distances. Similar long-range correlations have been documented in the cat retina [22].

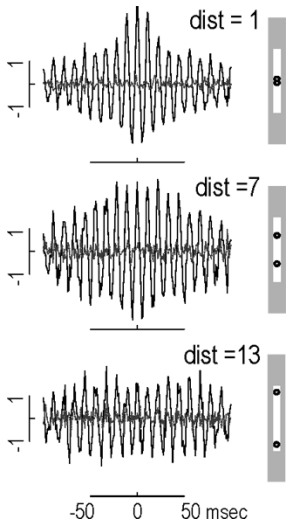

Fig. 3. HFOPs remain phase locked over long distances. CCHs between ganglion cell pairs arranged symmetrically about the center of a bar stimulus (see illustration to left of each plot). Center-to-center distance (dist) shown in upper right corner.

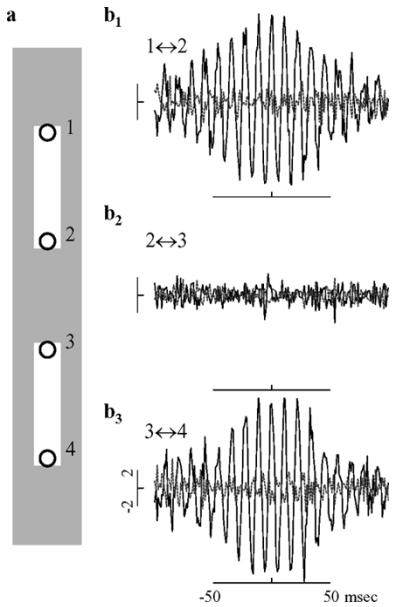

Fig. 4. HFOPs are stimulus specific for high-contrast features. (a) Location of stimuli (white rectangles) relative to the receptive field centers of recorded ganglion cells, labeled 1–4 (circles). (b1)—(b3) CCHs (solid black lines) and associated shift predictors (dashed gray lines) computed during the plateau portion of the response for pairs of ganglion cells at opposite ends of the same bar or at opposing tips of separate bars. All ganglion cell pairs were separated by 7-GC receptive field diameters. (b1) Pair $1 \leftrightarrow 2$ from upper bar (b2) Pair $2 \leftrightarrow 3$ from separate bars. (b3) Pair $3 \leftrightarrow 4$ from lower bar. Correlations were only significant between pairs from the same bar.

In a companion study [16], it was shown that HFOPs in the retina model depend critically on three elements that determined the gain and delay of the axon-mediated feedback loop, which are: 1) local excitation of axon-bearing amacrine cells via gap junctions with neighboring ganglion cells; 2) long-range feedback inhibition from the axon-bearing amacrine cells onto the surrounding ganglion cells; and 3) synaptic and conduction delays in the axon-mediated inhibitory feedback loop. Reducing by 50% the gap junction coupling strength from ganglion cells to neighboring axon-bearing amacrine cells, or the strength of long-range inhibitory feedback from the axon-bearing amacrine cells, completely eliminated the HFOPs evoked by weak full-field stimulation. The magnitude of the HFOPs evoked by large, high-contrast spots could also be strongly modulated by changing the axonal-conduction delay within physiologically reasonable bounds (i.e., within a few milliseconds).

B. Stimulus Specificity

We examined the stimulus specificity of the HFOPs evoked by two identical bars that were turned on simultaneously [Fig. 4(a)]. HFOPs were phase locked between regions responding to the same bar, but not between locations responding to different bars. CCHs obtained during the plateau portion of the response were plotted for ganglion cell pairs at opposite ends of the same bar (Fig. 4(b), upper bar; Fig. 4(b), lower bar), or at the nearest opposing tips of the two separate bars [Fig. 4(b)]. Even though the ganglion cells in each pair were separated by the same distance and were stimulated identically within their receptive field centers, only HFOPs within the same bar were strongly phase locked. The intensity of the two bar stimuli, equal to 0.5, corresponded to the maximum intensity examined and produced the strongest temporal correlations. In other experiments, similar or better stimulus specificity was present at lower bar intensities that evoked weaker HFOPs (not shown). The following experiments were mostly conducted with maximal intensity bars, as these provided the most stringent tests of stimulus specificity.

The degree of phase locking between the HFOPs evoked by spatially separate stimuli was examined systematically as a function of the distance separating two identical bars aligned end-to-end (Fig. 5). As measured by the CCHs between a fixed pair of model ganglion cells, HFOPs at the two recording sites were substantially phase locked when the opposing tips of the two bars were separated by a distance less than the diameter of a ganglion cell receptive field, but became largely independent at greater separations. Ganglion cells between the two stimuli were strongly suppressed by lateral inhibition and thus did not fire spikes, as shown by the spatial profile of the plateau firing rates along a vertical cross section passing down the central axis of the two stimuli.

The degree of phase locking between HFOPs evoked by separate bars was proportional to the activity of the neurons in the space between them. CCHs were recorded between a pair of ganglion cells responding to two separate bars while the cells in the region between them were stimulated at a lower or equal intensity (Fig. 6). Phase locking between HFOPs recorded at the two sites increased in proportion to the intensity of the stimulation in the connecting region. Phase locking between the two bars remained substantial as long as the stimulus intensity in the connecting region was at or above approximately 1/4 the intensity of the two bars. The spatial profile of the plateau firing rate along a vertical cross section passing through the main axis of the two stimuli revealed a relationship between the activity of the ganglion cells in the connecting region and the degree of phase locking between the two bars. HFOPs evoked by the two bars were mostly phase independent as long as the activity of the ganglion cells in the connecting region was below baseline levels.

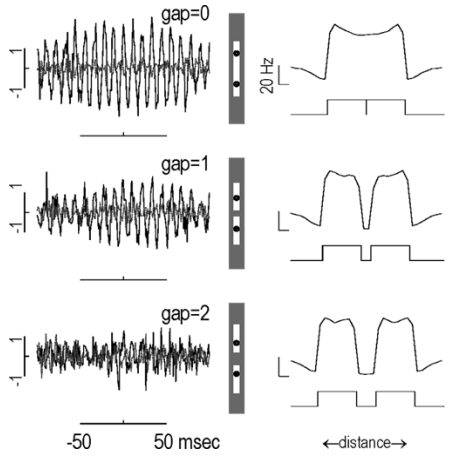

Fig. 5. Phase locking of HFOPs declines rapidly as the distance between spatially separate stimuli increases. Left column: plateau CCHs between a fixed pair of ganglion cells responding to two separate bars. The distance between the opposing ends of the two bars (gap) is indicated in the upper right of each plot. Correlations fall off rapidly with increasing separation. Right column: spatial profile of the plateau firing rate along a cross section through the central axis of the two stimuli. The plateau firing rates of the cells in the gap are very nearly zero.

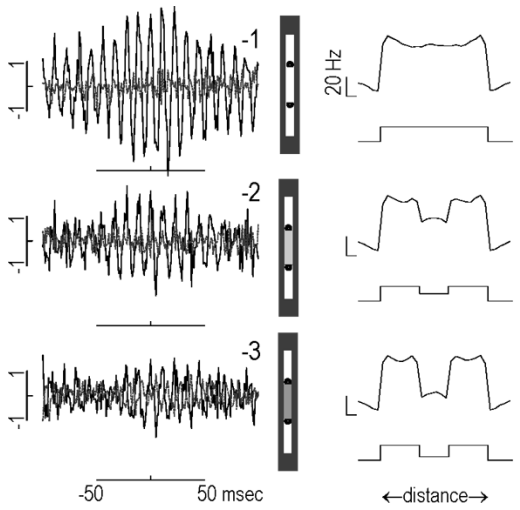

Fig. 6. Phase locking of HFOPs is proportional to the activity in the intervening region between spatially separate stimuli. Left column: plateau CCHs (solid black lines) and associated shift predictors (dashed gray lines) between a fixed pair of ganglion cells stimulated by two separate bars. The intensity of both bars was – 1 ($\log_2$ units) while cells in the gap between them were stimulated at an equal or lower intensity, indicated to the upper right of each plot. Phase locking increased steadily with gap intensity. Right column: spatial profile of plateau firing activity along a cross section through the principal axis of the two stimuli. The firing rate of ganglion cells in the gap was above or near baseline levels when stimulated by an intensity greater than approximately 1/4 that of the bars themselves, consistent with the gap intensity below which firing correlations become very weak.

To investigate the phase locking of HFOPs in continuously shaded regions, the intensity along a narrow bar was modulated in a sinusoidal fashion, thus producing two patches of elevated intensity in the absence of any abrupt high-contrast borders along the stimulus axis (Fig. 7). CCHs were computed between pairs of ganglion cells located at four equidistant points, chosen such that the local intensity within their receptive field centers equaled the average intensity over one cycle of the stimulus (half way between the maximum and minimum values).

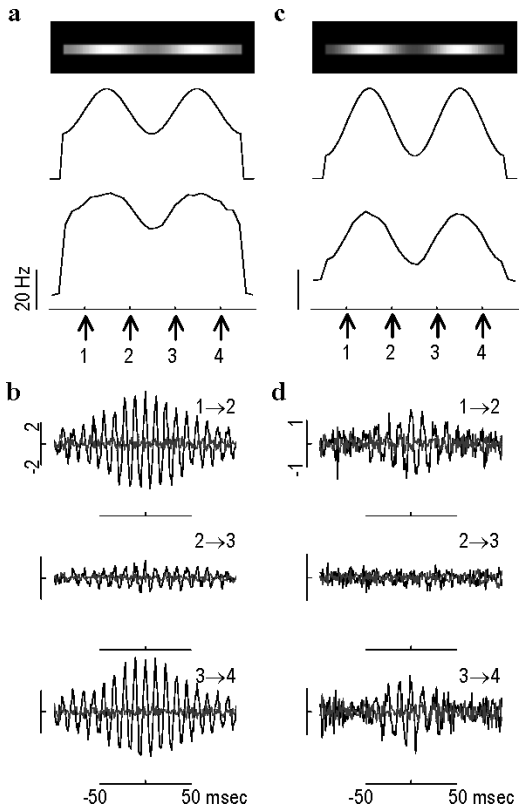

Fig. 7. Specificity of HFOPs between stimuli defined by shaded boundaries. (a) Top: sinusoidally modulating the intensity of a narrow bar produced two distinct patches. Middle: cross section of stimulus intensity profile. Bottom: plateau firing rates of cells along the axis of the bar stimulus. Arrows indicate the locations of four symmetrically-placed cells that received similar center stimulation. (b) CCHs between cell pairs denoted in denoted in panel (a). Cells responding to the same patch were more strongly correlated than cells responding to different patches. (c) and (d) Same organization as in (a), (b) except the depth of the sinusoidal modulation was increased, causing the firing correlations to become even more stimulus specific.

HFOPs were stimulus- specific even for relatively shallow intensity modulations and become progressively more so as the modulation depth increased. Thus, along a narrow contour, the phase locking behavior of model-generated HFOPs showed the same stimulus specificity for features defined by shaded boundaries as for features defined by sharp borders.

Many natural scenes contain overlapping objects separated by relatively low-contrast borders. To determine whether ganglion cells responding to such regions exhibit stimulus specificity similar to that present in their responses to narrow bars, we stimulated the model retina with a natural gray-scale image. To make the segmentation problem realistic, the image contained two natural objects (rats) of similar luminance whose profiles were partially overlapping [Fig. 8(a)]. To account for processing in the outer retina [5], the contrast of the original gray scale image was increased. The minimum intensity of the input image was set to 0.0 and the maximum intensity to 0.15. The plateau firing rates of the model ganglion cells, recorded for 10 s and averaged over 100 trials, yielded a reasonably good reproduction of the original high-contrast image [Fig. 8(b)]. A square, $9\sqrt{2}$ GC diameters on a side, was laid across the boundary between the two rats and representative ganglion cells located at the four vertices were used to assess the feature selectivity of their oscillatory responses. All four ganglion cells received approximately

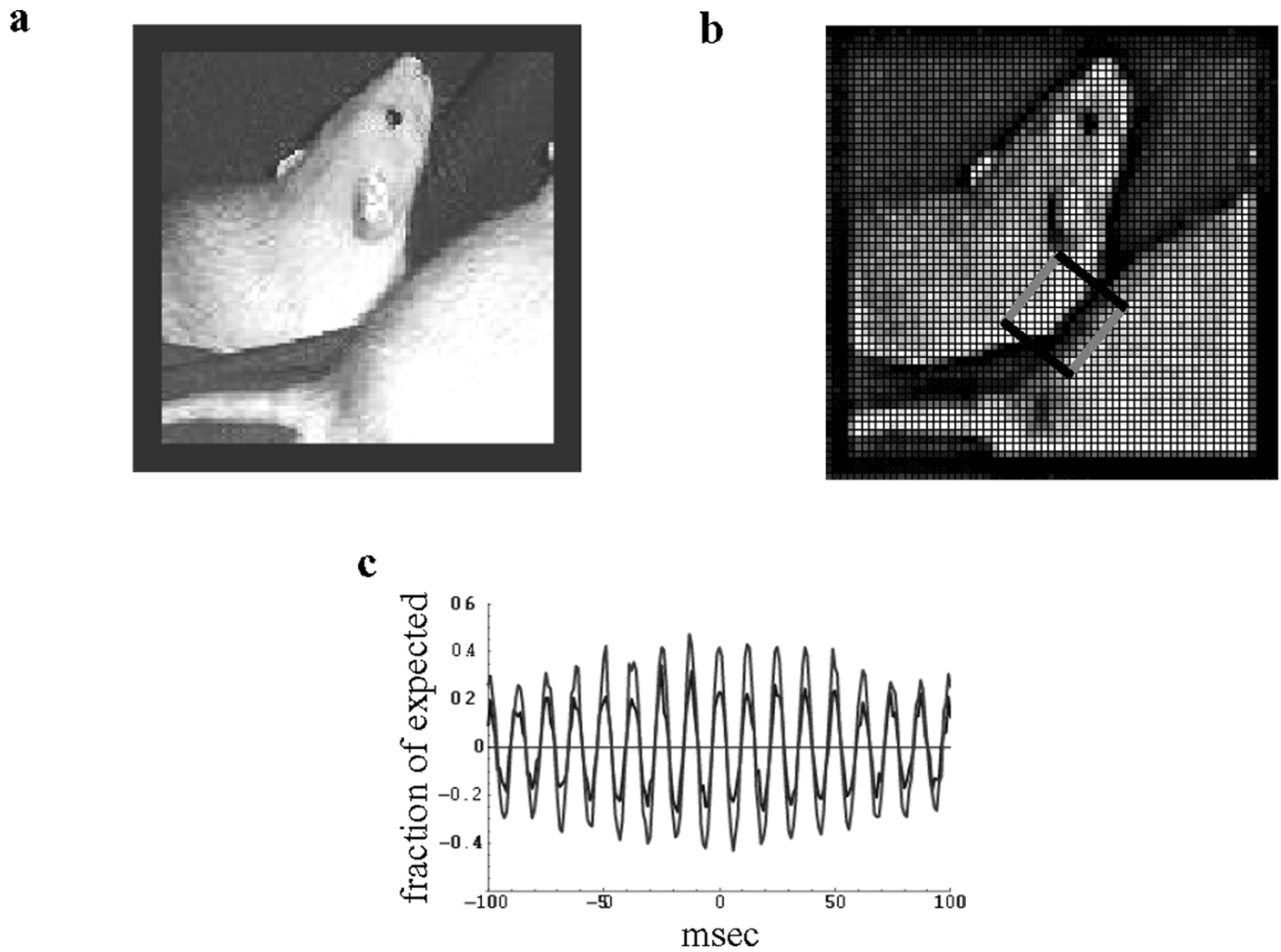

Fig. 8. HFOPs are less specific between overlapping objects in natural scenes. (a) High-contrast grayscale image containing two similar overlapping objects (rats) was used to stimulate the model retina (input image size: 128 × 128 pixels, minimum intensity: 0.0, maximum intensity: 0.15). (b) Plateau firing rates of each ganglion cell plotted as a 2-D image. The average firing rates reproduced the gray-scale features of the original image (plateau period began 200 ms after stimulus onset and lasted for 10 s, 100 trials, output image size: 64 × 64 GCs). (c) HFOPs were only partially stimulus specific. Correlations were computed between ganglion cells located at the vertices of a square [see panel (b)], either responding to the same rat [gray trace in panel (c), gray lines in panel (b) or to different rats (black trace in panel (c), black lines panel (b)]. Cell pairs responding to the same rat were more strongly correlated than cells pairs responding to separate rats, though all pairs were separated by an equal distance and had similar firing rates (starting with the cell at 6 o'clock and moving counterclockwise, the rates were 23.5, 22.2, 24.6, 24.6 Hz, respectively). Shift predictors were negligible and were not subtracted for these experiments. Correlations expressed as a fraction of the expected synchrony during the response.

equal center stimulation and their plateau firing rates differed by no more than 11%. Similar results were obtained with other ganglion cell pairs (not shown). HFOPs in this example were not as stimulus specific as the oscillations produced by narrow bars, although ganglion cells responding to the same rat (gray trace; Fig. 8(c) were still more correlated than were ganglion cells responding to different rats (black trace; Fig. 8(c). The average synchrony between the two pairs of ganglion cells responding to the same rat was 0.42 while the average for cells responding to different rats was 0.23.

IV. Discussion

A. Stimulus-Specific HFOPs Arise Naturally From Retinal Circuitry

HFOPs are ubiquitous in the vertebrate retina. One clue to their function is the strong stimulus specificity exhibited by HFOPs recorded simultaneously at separate retinal locations. Here, we have used a computer model to explore the circuitry underlying the phase locking behavior of retinal HFOPs produced by axon-mediated feedback. HFOPs produced by axon-mediated feedback were of the same general frequency, amplitude, and duration as measured by the persistence of side-peaks in the CCH, as HFOPs recorded experimentally. Moreover, our results suggest that retinal patterns of connectivity may have evolved so that HFOPs are most strongly phase locked between connected regions responding to the same stimulus. Given the high level of synaptic noise in the model, the principal characteristics of phase locking behavior reported here should reflect general dynamical properties of the axon-mediated feedback circuit rather than precise details of the implementation.

Model generated HFOPs recorded at separate retinal locations were phase locked whenever there was a continuous path of stimulated cells joining them. This finding suggests that the one topological parameter encoded by phase locked HFOPs is connectedness. In principle, topological information encoded

by the degree of phase locking between retinal HFOPs could be read out by downstream neurons. For example, HFOPs arising from simply connected regions of the visual space would add in phase, and thus might produce larger responses than HFOPs arising from nonconnected regions, which would add with random phase. Sensitivity to synchronous input has been demonstrated in visual cortical neurons [1], suggesting that retinal HFOPs might contribute to the detection of contiguous features. Retinal HFOPs may also influence the development of intracortical connections via spike-timing-dependent-plasticity (STDP) [29]. By causing regions responding to the same object to oscillate in phase, retinal HFOPs may contribute to the development of appropriate feature detectors in the visual cortex.

When bar stimuli were moved apart by more than one ganglion cell receptive field center diameter, their HFOPs were no longer appreciably phase locked, even at separations for which there would still have been long range axonal fibers crossing between them. The sharp fall off in phase locking with increasing separation is consistent with a dependence on gap junctions, which necessarily only link nearest neighbors. In contrast, the long range of axon-mediated inhibition interactions is incommensurate with a sharp dependence on separation distance. Previous theoretical work has demonstrated that gap junctions, due to their low-pass temporal filter characteristics, cause action potentials to be strongly attenuated [15]. Thus, spikes cannot be passively propagated through chains of gap junctions, and instead must be boosted by firing events along the chain to be reliably transmitted. Due to lateral inhibition, spatially separate stimuli tend to be surrounded by halos of suppressed activity, which in turn act to block to propagation of spikes through the chains of gap junctions. This block can be relieved, however, by stimulating the intervening cells sufficiently to bring them near threshold. Here, a sufficiently high level of firing for propagating phase information through local connections was on the order of the background activity.

B. Experimental Predictions

The main prediction of the model is that the specificity of HFOPs will depend very sharply on the spatial separation between two stimuli. In particular, phase locking is predicted to fall off rapidly as the two stimuli are separated by more than one receptive field diameter. Such a sharp spatial dependence is inconsistent with the long-range projections of axon-bearing amacrine cells and instead highlights the critical role of gap junctions in synchronizing HFOPs within contiguous regions. An experimental evaluation of how phase locking between retinal locations activated by spatially separate stimuli depends on the distance between them can thus provide important insights into the physiological mechanisms underlying HFOPs.

The model also predicts that HFOPs recorded at separate retinal locations can remain strongly phase locked even when the region between them is not stimulated uniformly. Rather, the model requires only that for appreciable phase locking to be present, there exist a contiguous path, or paths, connecting the two regions along which sufficient stimulation is present to maintain firing activity at or above baseline levels. The prediction that strong phase locking requires at least some firing activity in the intervening region is consistent with a dependence on axon-mediated inhibition from spiking amacrine cells as well as the need to boost signals transmitted through serial chains of gap junctions.

Finally, the proposed model suggests that for some stimulus configurations strong specificity will break down, particularly stimuli sharing a long parallel interface likely to be bridged by large numbers of connecting axons. Thus, the degree of phase locking between nearby stimuli is likely to depend on a combination of the distance between them and on the total length of their nearest opposing borders.

REFERENCES

[1] J. M. Alonso, W. M. Usrey, and R. C. Reid, "Precisely correlated firing in cells of the lateral geniculate nucleus," *Nature*, vol. 383, pp. 815–819, 1996.

[2] M. Ariel, N. W. Daw, and R. K. Rader, "Rhythmicity in rabbit retinal ganglion cell responses," *Vis. Res.*, vol. 23, pp. 1485–1493, 1983.

[3] M. Castelo-Branco, S. Neuenschwander, and W. Singer, "Synchronization of visual responses between the cortex, lateral geniculate nucleus, and retina in the anesthetized cat," *J. Neurosci.*, vol. 18, pp. 6395–6410, 1998.

[4] O. D. Creutzfeldt, B. Sakmann, H. Scheich, and A. Korn, "Sensitivity distribution and spatial summation within receptive-field center of retinal on-center ganglion cells and transfer function of the retina," *J. Neurophysiol.*, vol. 33, pp. 654–671, 1970.

[5] D. Dacey, O. S. Packer, L. Diller, D. Brainard, B. Peterson, and B. Lee, "Center surround receptive field structure of cone bipolar cells in primate retina," *Vis. Res.*, vol. 40, pp. 1801–1811, 2000.

[6] D. M. Dacey and S. Brace, "A coupled network for parasol but not midget ganglion cells in the primate retina," *Vis. Neurosci.*, vol. 9, pp. 279–290, 1992.

[7] F. D. Carli, L. Narici, P. Canovaro, S. Carozzo, E. Agazzi, and W. G. Sannita, "Stimulus- and frequency-specific oscillatory mass responses to visual stimulation in man," *Clin. Electroencephalogr.*, vol. 32, pp. 145–151, 2001.

[8] M. A. Freed, "Rate of quantal excitation to a retinal ganglion cell evoked by sensory input," *J. Neurophysiol.*, vol. 83, pp. 2956–2966, 2000.

[9] M. A. Freed and P. Sterling, "The ON-alpha ganglion cell of the cat retina and its presynaptic cell types," *J. Neurosci.*, vol. 8, pp. 2303–2320, 1988.

[10] L. J. Frishman, A. W. Freeman, J. B. Troy, D. E. Schweitzer-Tong, and C. Enroth-Cugell, "Spatiotemporal frequency responses of cat retinal ganglion cells," *J. General Physiol.*, vol. 89, pp. 599–628, 1987.

[11] L. J. Frishman, S. Saszik, R. S. Harwerth, S. Viswanathan, Y. Li, E. L. Smith 3rd, J. G. Robson, and G. Barnes, "Effects of experimental glaucoma in macaques on the multifocal ERG. Multifocal ERG in laser-induced glaucoma," *Doc. Ophthalmol.*, vol. 100, pp. 231–251, 2000.

[12] G. L. Gerstein and D. H. Perkel, "Mutual temporal relationships among neuronal spike trains. Statistical techniques for display and analysis," *Biophys. J*, vol. 12, pp. 453–473, 1972.

[13] H. Ishikane, A. Kawana, and M. Tachibana, "Short- and long-range synchronous activities in dimming detectors of the frog retina," *Vis. Neurosci.*, vol. 16, pp. 1001–1014, 1999.

[14] R. Jacoby, D. Stafford, N. Kouyama, and D. Marshak, "Synaptic inputs to ON parasol ganglion cells in the primate retina," *J. Neurosci.*, vol. 16, pp. 8041–8056, 1996.

[15] G. T. Kenyon and D. W. Marshak, "Gap junctions with amacrine cells provide a feedback pathway for ganglion cells within the retina," in *Proc. R Soc. Lond. B Biol. Sci.*, vol. 265, 1998, pp. 919–925.

[16] G. T. Kenyon, B. Moore, J. Jeffs, K. S. Denning, G. S. Stephens, B. J. Travis, J. S. George, J. Theiler, and D. W. Marshak, "A model of high frequency oscillatory potentials in retinal ganglion cells," Vis. Neurosci., 2003, to be published.

[17] G. T. Kenyon, K. R. Moore, and D. W. Marshak, "Stimulus-specific synchrony between alpha ganglion cells in a computer model of the mammalian retina," *Soc. Neurosci.*, vol. 25, pp. 1042–1042, 1999.

[18] H. Kolb and R. Nelson, "OFF-alpha and OFF-beta ganglion cells in cat retina: II. Neural circuitry as revealed by electron microscopy of HRP stains," *J. Comparative Neurol.*, vol. 329, pp. 85–110, 1993.

[19] M. Laufer and M. Verzeano, "Periodic activity in the visual system of the cat," *Vis. Res.*, vol. 7, pp. 215–229, 1967.

[20] D. N. Mastronarde, "Correlated firing of retinal ganglion cells," *Trends. Neurosci.*, vol. 12, pp. 75–80, 1989.

[21] S. Neuenschwander, M. Castelo-Branco, and W. Singer, "Synchronous oscillations in the cat retina," *Vis. Res.*, vol. 39, pp. 2485–2497, 1999.
[22] S. Neuenschwander and W. Singer, "Long-range synchronization of oscillatory light responses in the cat retina and lateral geniculate nucleus," *Nature*, vol. 379, pp. 728–732, 1996.
[23] N. V. Rangaswamy, D. C. Hood, and L. J. Frishman, "Regional variations in local contributions to the primate photopic flash ERG: Revealed using the slow-sequence mfERG," *Invest Ophthalmol. Vis. Sci.*, vol. 44, pp. 3233–3247, 2003.
[24] R. H. Steinberg, "Oscillatory activity in the optic tract of cat and light adaptation," *J. Neurophysiol.*, vol. 29, pp. 139–156, 1966.
[25] J. B. Troy, J. K. Oh, and C. Enroth-Cugell, "Effect of ambient illumination on the spatial properties of the center and surround of Y-cell receptive fields," *Vis. Neurosci.*, vol. 10, pp. 753–764, 1993.
[26] D. I. Vaney, "Patterns of neuronal coupling in the retina," in *Prog. Retinal Eye Res.*, vol. 13, 1994, pp. 301–355.
[27] L. Wachtmeister, "Oscillatory potentials in the retina: What do they reveal," in *Prog. Retinal Eye Res.*, vol. 17, 1998, pp. 485–521.
[28] L. Wachtmeister and J. E. Dowling, "The oscillatory potentials of the mudpuppy retina," *Invest Ophthalmol. Vis. Sci.*, vol. 17, pp. 1176–1188, 1978.
[29] H. Yao and Y. Dan, "Stimulus timing-dependent plasticity in cortical processing of orientation," *Neuron*, vol. 32, pp. 315–323, 2001.

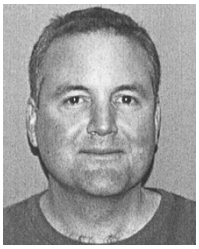

Garrett T. Kenyon received the B.A. degree in physics from the University of California, Santa Cruz, in 1984, and the M.S. and Ph.D. degrees in physics from the University of Washington, Seattle in, 1986 and 1990, respectively.

He received further Post-Doctoral training at the Division of Neuroscience, Baylor College of Medicine, Houston, TX, and at the Department of Neurobiology and Anatomy, University of Texas Medical School, Houston, the later under the supervision of Prof. Marshak. He has been a Staff Member in the Biological and Quantum Physics Group, Los Alamos National Laboratory, Los Alamos, NM, since 2001. His research interests involve the application of computational and theoretical techniques to the analysis of computation in biological neural networks.

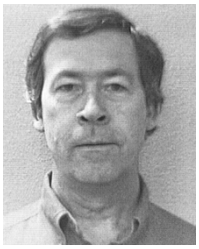

Bryan J. Travis received the A.B. degree in mathematics and physics from the University of Alabama, Huntsville, in 1968, and the Ph.D. degree in applied mathematics from Florida State University, Tallahassee, in 1974.

He worked for the Boeing Company Aerospace Division, in 1967–1968, and the Florida University System from 1968–1974. He has been a Staff Member at Los Alamos National Laboratory, Los Alamos, NM, since 1974, where he is presently in the Earth and Environmental Sciences Division. He has published in a variety of areas of computational physics, including geophysical fluid dynamics, Boltzmann transport equations, electromagnetic sensing, microbial ecology, and computational neurobiology. His research interests include large-scale computational modeling of neurobiological systems and inverse problem methodologies.

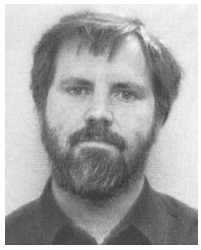

James Theiler received the Ph.D. degree in physics from the California Institute of Technology, Pasadena, in 1988, with a thesis on characterizing chaotic time series.

He worked as a Post-Doc at the Institute for Nonlinear Science, University of California, San Diego, as a Staff Member at MIT Lincoln Laboratory, and as a Post-Doc with half-time appointments at the Santa Fe Institute and the Complex Systems Group, Los Alamos National Laboratory, Los Alamos, NM. He is currently a Staff Member in the Space and Remote Sensing Sciences Group, Los Alamos National Laboratory. His research interests include statistical and computational issues in the analysis and understanding of data.

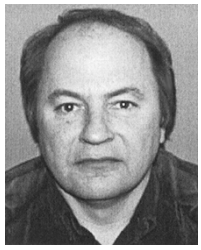

John S. George received the Ph.D. degree in physiology from Vanderbilt University, Nashville, TN, based on dissertation studies at the National Institutes of Health, Bethsada, MD.

He then took Post-Doctoral and Staff Positions at the Los Alamos National Laboratory, Los Alamos, NM, in the Life Sciences and Physics Divisions. The principal theme of his work has been functional neuroimaging. He has been involved in experimental studies as well as the development of analytical and modeling techniques for magnetoencephalography (MEG), the development and application of optical methods for functional neuroimaging, and the development of instrumentation for very low-field MRI.

Gregory J. Stephens received the Ph.D degree in physics from the University of Maryland, College Park, in 2000 with a thesis on the nonequilibrium dynamics of phase transitions.

From 2000 to 2001, he worked as a postdoc in cosmology at Los Alamos National Laboratory (LANL), Los Alamos, NM. In 2001, he changed research directions to focus on fundamental problems in computational and theoretical neuroscience and is currently a postdoc in the Biophysics and Quantum Physics Group at LANL. His research interests center on understanding the complex and powerful computations achieved by neural systems.

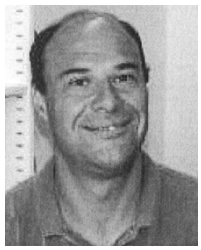

David W. Marshak received the B.A. degree (with honors) in anthropology from Cornell University, Ithaca, NY, in 1975, and the Ph.D. degree in anatomy from the University of California, Los Angeles (UCLA), in 1982.

He continued his training as a Post-Doctoral Fellow at the Biological Laboratories, Harvard University, Cambridge, MA, and a Grass Foundation Fellow in Neurophysiology at the Marine Biologícal Laboratory. In 1984, he joined the faculty of the Department of Neurobiology and Anatomy, University of Texas Medical School, Houston. He has been there ever since and is now a Full Professor. The research goals of his laboratory are to learn how neural circuits in the primate retina accomplish parallel processing of images and, ultimately, to use such knowledge to design better artificial visual systems.